



Contents lists available at ScienceDirect

## Composites Science and Technology

journal homepage: [www.elsevier.com/locate/compscitech](http://www.elsevier.com/locate/compscitech)

## Optimal design of sandwich panels made of wood veneer hollow cores

S. Banerjee<sup>a,\*</sup>, D. Bhattacharyya<sup>b</sup><sup>a</sup> Centre of Excellence in Engineered Fibre Composites, Faculty of Engineering & Surveying, University of Southern Queensland, Toowoomba, Old 4350, Australia<sup>b</sup> Centre for Advanced Composite Materials, Department of Mechanical Engineering, The University of Auckland, Private Bag 92019, Auckland, New Zealand

## ARTICLE INFO

## Article history:

Received 26 May 2010

Received in revised form 9 December 2010

Accepted 10 December 2010

Available online xxxx

## Keywords:

- A. Hollow core
- A. Wood veneer
- C. Sandwich structures
- C. Failure criteria
- C. Optimisation

## ABSTRACT

In response to the growing interest in replenishable, lightweight, stiff and strong materials, a novel sandwich panel with a hollow core has been manufactured using commercially produced 3-ply veneer. In this paper, the out-of-plane shear behaviour of the novel hollow core is analysed and the expressions for the failure loads are developed. A strength-based optimisation problem is formulated for predicting the optimum values of the panel dimensions that would produce minimum panel weight when subjected to bending. It has been found that the minimum weight, as predicted by the full four-parameter optimisation, is slightly lower than that obtained by using the closed form expressions derived on the basis of simplified three-parameter optimisation. Relationships between the active failure modes are explored. Design maps are shown for a wide range of loading that can be used to calculate the minimum panel weight and the corresponding values of the geometric parameters. The approach developed is general and is equally applicable for sandwich panels with similar hollow cores made of other materials.

© 2010 Elsevier Ltd. All rights reserved.

## 1. Introduction

Sandwich structures, originally developed and used in aerospace industries, have found applications in marine, automotive and sports goods industries. Typical sandwich structures are made of a low density core material bonded with thin, strong skins at top and bottom. While the skins are solid materials, cellular materials including balsa wood, manmade metallic, paper, ceramic and thermoplastic honeycombs, polymeric and metallic foams are popular as core materials. Apart from the excellent stiffness and strength to weight ratios, cellular cores are attractive due to their good thermal and/or acoustic insulation, and energy absorbing capabilities.

In conjunction with the experimental investigation of the development of new materials and topologies for cellular materials, theoretical/computational research has been concentrated on how to calculate their effective mechanical properties in terms of the topology, cell geometry and elastic properties of the cell wall material. The problem becomes more complicated for honeycomb cores as the skin affects the core deformation at the skin–core interface.

Kelsey et al. [1] used strain energy method for predicting the upper and the lower bounds on the effective transverse shear moduli of honeycombs. Gibson and Ashby [2] applied the mechanics of materials and the energy method for determining the transverse shear stiffness of hexagonal core. Penzien and Didriksson [3] used a displacement field for incorporating warping of the cell walls produced by the skin. The homogenisation approach for periodic media

was used by Shi and Tong [4] to evaluate the expressions for out-of-plane shear moduli of honeycombs. Using a similar approach, Xu et al. [5] presented formulae of equivalent stiffnesses for common cellular cores. Hohe and Becker [6,7] used a homogenisation approach based on the equivalence of strain energy and developed expressions for the effective elastic constants of several core topologies. Chen and Davalos [8] incorporated the effect of skin, and presented an explicit analytical model for calculating the stiffness and stress distributions in the honeycomb cell walls. Among the numerical approaches, Grediac [9] determined the transverse shear moduli of honeycombs, by analysing a representative unit cell using the finite element method. Though a number of articles on the estimation of the out-of-plane stiffness parameters of cellular cores are available, few address the out-of-plane strength properties. Zhang and Ashby [10] developed expressions for the failure loads of honeycombs under transverse compression and shear loading and compared with the experimental results for Nomex honeycombs.

Performance optimisation of metallic sandwich panels and plates with various cores has been widely explored. For example, optimisation of metallic sandwich plates with truss cores by Wicks and Hutchinson [11,12], design of metallic sandwich panels with textile cores [13], pyramidal truss cores [14] by Zok et al. and corrugated cores by Valdevit et al. [15]. Rathbun et al. [16] developed a general methodology for the weight optimisation of metallic sandwich panels subjected to bending loads. Wei et al. [17] showed that the optimised performances of the prismatic cores are comparable to that of a honeycomb core. Furthermore, Cote et al. [18] analysed the compressive and shear behaviour of corrugated and diamond lattice materials. Extensive study of

\* Corresponding author. Tel.: +61 7 4631 1325; fax: +61 7 4631 2526.

E-mail address: [Sourish.Banerjee@usq.edu.au](mailto:Sourish.Banerjee@usq.edu.au) (S. Banerjee).

mechanical behaviour of sandwich structures can be found in the classic book by Allen [19], monographs of Zenkert [20] and Vinson [21], review article on various computational models for sandwich panels and shells by Noor et al. [22] and the references thereof.

With the worldwide interest in replenishable and biodegradable materials, a corrugated profile has been successfully manufactured by roll forming and matched-die forming of commercially available 3-ply veneer sheets [23]. Wood veneers are obtained from Radiata Pine trees of New Zealand and are generally considered to be replenishable, with the advantage of being lightweight as well. For the present work, these profiles were adhesively bonded in the out-of-plane mode to produce a novel multiple corrugated core (referred to as ‘hollow core’) which was glued to veneer sheets at the top and bottom, Fig. 1a. The average density of the core is  $118 \text{ kg/m}^3$ , a 77% reduction from the veneer density of  $520 \text{ kg/m}^3$ . The flexibility of the manufacturing process of the core allows a wide range of cell geometry to be produced, giving the possibility of tailoring the cell structure and the panel geometry to achieve optimal performance for specific materials and end usages. This study focuses on developing a methodology for predicting the optimum values of the geometrical parameters of the panel that would lead to minimum panel weight. The panel subjected to bending load is considered as the loading case. Because the core is subjected to out-of-plane shear forces due to the bending of the sandwich panel, the out-of-plane shear behaviour of the new core material is analysed first. For this purpose, the microstructure is modelled at the mesoscale, i.e. at the cell level. Failure criteria of the whole panel are then developed for optimisation. Strength-based design is chosen as it is more important from the design point of view and is suitable for higher loads. Based on the optimisation results, design maps are generated that can be used to calculate the optimal geometrical parameters and weight of the sandwich panel for a wide range of loading.

## 2. Out-of-plane shear behaviour of the hollow core

The plan view of the hollow profile is shown in Figs. 1b and 2. Geometry of the core can be characterised in terms of the radius

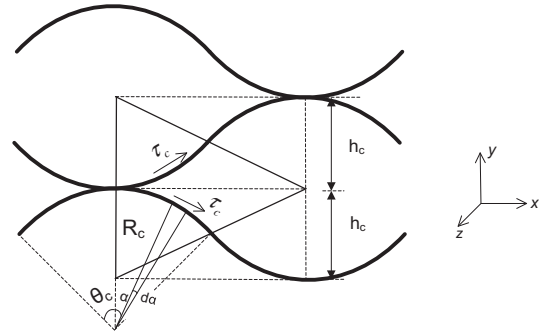


Fig. 2. A unit cell, along with the shear stresses acting in the cell walls, is shown. The triangle is the effective area of the unit cell.

$R_c$ , depth of the half cell  $h_c$ , half angle  $\theta_c$  and thickness of the cell wall  $t_c$ ; subscript ‘c’ denotes core. As  $R_c(1 - \cos \theta_c) = h_c/2$ , the effective mechanical properties of the core become functions of two independent geometric parameters,  $t_c/R_c$  and  $\theta_c$ . For a quarter of a cell, the unit cell (the triangle in Fig. 2) has an area of  $2h_c R_c \sin \theta_c$ . Therefore, for thin cell walls,  $4R_c^2(1 - \cos \theta_c) \sin \theta_c \rho^* = 2R_c \theta_c t_c \rho_c$ , where,  $\rho_c$  and  $\rho^*$  are the densities of the cell wall material and the hollow core, respectively. Simplification of the above relationship, leads to an approximate expression of the relative density  $\phi$  of the hollow core as (for  $\phi \ll 1$ )

$$\phi = \frac{\rho^*}{\rho_c} = \frac{1}{2} \frac{t_c}{R_c} \frac{\theta_c}{(1 - \cos \theta_c) \sin \theta_c}. \quad (1)$$

The main assumption for the analysis of sandwich structures under bending loads is that the faces carry all the flexural stresses and the core carries all the out-of-plane shear stresses. When subjected to out-of-plane shear forces, the deformation and hence, the stress distribution in a cell wall is affected not only by its interconnecting neighbours, but also by the strain compatibility condition at the interface of the face and core. This results in a very complicated stress distribution in the cell walls. In this work, neglecting skin effect, the core stresses are determined based on the force equilibrium condition, in the middle of the core (away from the faces).

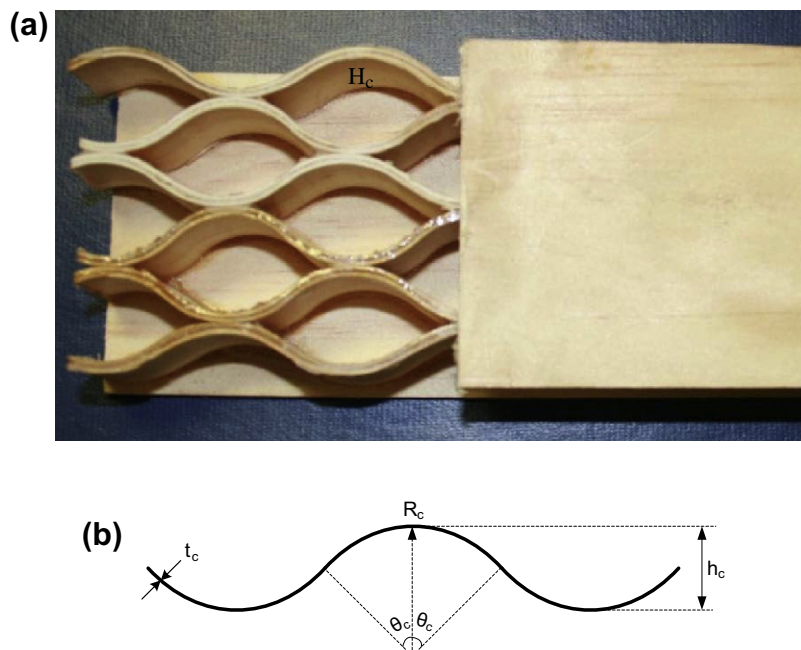


Fig. 1. (a) A typical sandwich panel made with hollow core and face sheets made of 3-ply veneer. (b) The geometric parameters characterising the hollow core in the plane of paper.

The cell wall material is made of 3-ply veneer adhesively bonded together at  $0^\circ/90^\circ/0^\circ$ , where  $0^\circ$  denotes the longitudinal grain direction of a single ply. Experimental observations show that during forming and under loading, relative movement between the layers is negligible, except at very high strains. Therefore, the cell wall material could be considered as homogeneous and linear elastic. The tensile test measurement on 3-ply veneer specimen shows that the average ratio of the Young's moduli of the veneer in the  $0^\circ$  and  $90^\circ$  directions is about 1.34 [23], allowing the cell wall material to be considered quasi-isotropic. Though the cell wall material in this study is veneer, the analysis presented is independent of the material chosen and is equally applicable to similar hollow cores made of other materials. Complete cells are shown in Fig. 1a with depth  $H_c$  in the  $z$ -direction. For the analysis purpose, a quarter of a cell is chosen as a *unit cell* as shown in Fig. 2, taking into account of the periodicity and symmetry of the structure. The unit cell is made of two cell walls of half length connected at a node, with each cell wall modelled as a thin shell. Mechanics of the core is now analysed to (i) develop a relationship between the external shear force and the shear stress at the cell level, and (ii) calculate the critical shear force that causes cell wall buckling. Let the external shear stress acting on the unit cell be  $V/H_c$ , where the shear force  $V$  per unit width is applied in the principal direction  $x$ . The shear stress in the  $x$ -direction has been analysed here as the core is stiffer in this direction. However, similar analysis can be performed for shear force applied in the  $y$ -direction as well. Because of thin cell walls, the shear stress distribution is considered uniform across the cell wall thickness, and let the shear stress acting in each cell wall be  $\tau_c$ . Considering force equilibrium in the  $x$ -direction (refer to Fig. 2),

$$\frac{V}{H_c} 4R_c^2 (1 - \cos \theta_c) \sin \theta_c = \int_0^{\theta_c} 2\tau_c t_c R_c \cos \alpha d\alpha. \quad (2)$$

Simplifying Eq. (2), the following expression is obtained

$$\tau_c = 2 \frac{V}{H_c} \frac{R_c}{t_c} (1 - \cos \theta_c). \quad (3)$$

The cell wall buckling, when subjected to shear loading, can be explored in the following manner. Each cell wall is made of two curved shells joined at the point of contra flexure. Hence, for the half cell wall, the radial displacement and the bending moment vanish along the line passing through the point of contra flexure; thus that edge can be considered as simply supported. The boundary condition at the other edge lies in between "simply supported" and "fixed", but for conservative design, this edge has been assumed to be simply supported. Though the top and bottom edges are rigidly bonded with the faces, they are also assumed as simply supported. Therefore, the half cell wall has all the four edges simply supported and the *lower bound* of the critical buckling load is calculated (neglecting postbuckling). This would perhaps take into account of the imperfections due to the manufacturing defects of the hollow core structure. The critical buckling stress in a cell wall has been calculated based on the stated assumptions using [24]

$$\tau_{cr} = \left( \frac{f_1 \pi^2}{3} \right) \frac{E_c}{1 - \nu_c^2} \frac{t_c^2}{R_c^2} \theta_c^{-2}, \quad (4)$$

where  $E_c$  and  $\nu_c$  are the Young's modulus and the Poisson's ratio of the cell wall material, respectively. The value of factor  $f_1$  depends on the value of  $(\theta_c/\pi)(t_c/R_c)^{-1/2} \sqrt{[4]12(1 - \nu_c^2)}$ .

### 3. Failure criteria for the sandwich panel

Geometry of a sandwich panel can be completely described by the following independent geometrical parameters: for core  $t_c/R_c$ ,

$\theta_c$ ,  $H_c$ , for face sheet–thickness  $t_f$ , and density  $\rho_f$ . The self-weight (per unit area) of the panel can be expressed as

$$W = \frac{1}{2} \frac{t_c}{R_c} \frac{\theta_c}{(1 - \cos \theta_c) \sin \theta_c} \rho_c H_c + 2\rho_f t_f. \quad (5)$$

Let the sandwich panel be subjected to a maximum bending moment  $M$  and a maximum shear force  $V$  (both per unit width). As strength-based design is chosen here, the failure criteria are developed based on the failure modes. When subjected to bending, the possible failure modes of sandwich panel are as follows:

#### 3.1. Fracture of the face sheet (FF)

The flexural stress carried by the face is given by Zenkert [20],  $\frac{M}{t_f H_c}$ , for  $t_f \ll H_c$ . The face will not fracture if

$$\frac{M}{t_f H_c} \leq \sigma_f; \quad (6)$$

where  $\sigma_f$  is the fracture stress of the face material.

#### 3.2. Face wrinkling (FW)

To prevent wrinkling failure,

$$\frac{M}{t_f H_c} \leq \sigma_{wr}; \quad (7)$$

condition must be satisfied. Approximate expression for wrinkling stress  $\sigma_{wr}$  has been used from Niu and Talreja's work [25], after neglecting higher order terms,

$$\sigma_{wr} = \left( \frac{3E_c^*}{2(1 + \nu_c^*)(3 - \nu_c^*)} \right)^{2/3} (E_f)^{1/3};$$

where  $E_f$  is the Young's modulus of the face sheet,  $E_c^*$  and  $\nu_c^*$  are the out-of-plane Young's modulus and the Poisson's ratio of the core, respectively.  $E_c^*$  can be evaluated using the expression of Zhang and Ashby [10]  $E_c^* = \phi E_c$ .

#### 3.3. Core shear fracture (CF)

To prevent cell wall fracture, shear stress in the cell wall  $\tau_c$  (using Eq. (3)) must not exceed the maximum allowable shear stress of the cell wall,  $\tau_{max}$ , i.e.

$$\tau_c = 2 \frac{V}{H_c} \frac{R_c}{t_c} (1 - \cos \theta_c) \leq \tau_{max}. \quad (8)$$

#### 3.4. Core buckling (CB)

To prevent cell wall buckling failure, shear stress in the cell wall must not exceed the critical buckling stress,  $\tau_{cr}$ , given by Eq. (4). Therefore,

$$\tau_c = 2 \frac{V}{H_c} \frac{R_c}{t_c} (1 - \cos \theta_c) \leq \left( \frac{f_1 \pi^2}{3} \right) \frac{E_c}{1 - \nu_c^2} \frac{t_c^2}{R_c^2} \theta_c^{-2}. \quad (9)$$

Apart from the mentioned four failure criteria, *intracellular buckling* is another possible failure mode. Considering the radius of the inscribed circle in a cell as  $h_c$  (refer to Fig. 2), this failure criterion is given by [20]

$$\frac{M}{t_f H_c} \leq \frac{2E_f}{(1 - \nu_f^2)} \left( \frac{t_f}{4R_c(1 - \cos \theta_c)} \right)^2; \quad (10)$$

where  $\nu_f$  is the Poisson's ratio of the face sheet material.

#### 4. The optimisation problem

The aim of the panel optimisation is to predict the lowest weight of the sandwich panels and the corresponding values of the geometrical parameters, when the panel is subjected to a prescribed bending load. Therefore, the objective function is the panel self-weight and the failure criteria developed in Section 3 are the constraints for the optimisation. Non-dimensional load index for generalised bending of sandwich panels can be conveniently expressed by combining the maximum bending moment  $M$  and maximum shear force  $V$  (both per unit width) as  $\Pi = \frac{V^2}{EM}$  (from Ashby et al.'s work [26]) and  $l \equiv \frac{M}{V}$  is the characteristic length scale [11]. For four point bending of the sandwich panel,  $l = L/2$ , where,  $L$  is the span length. The normalised geometric parameters are  $\lambda_f = t_f/l$ ,  $\lambda_c = H_c/l$ ,  $t_c/R_c$  and  $\theta_c$ . As  $t_c/R_c$  ratio is an important parameter for the core, analogous to  $t_c/l_c$  ratio for the hexagonal core ( $l_c =$  length of the cell wall) [2], it has been kept unchanged. Alternatively,  $\lambda_{t_c}/\lambda_{R_c}$  can be used by normalising both the numerator and the denominator. Because the face and the core are made of the same material,  $E_f$  and  $E_c$ ,  $\nu_f$  and  $\nu_c$ ,  $\rho_f$  and  $\rho_c$  are replaced by  $E$ ,  $\nu$  and  $\rho$  respectively. The weight index  $w$  can be expressed as  $w = W/\rho l$  from [26]. Therefore, from (5), the weight index  $w$  of the sandwich panel can be expressed as

$$w = \frac{1}{2} \frac{t_c}{R_c} \frac{\theta_c}{(1 - \cos \theta_c) \sin \theta_c} \lambda_c + 2\lambda_f. \quad (11)$$

The failure criteria Eqs. (6)–(9) may now be expressed in the following forms:

$$\prod \lambda_f^{-1} \lambda_c^{-1} (\sigma_f/E)^{-1} \leq 1 \quad (\text{FF}) \quad (12a)$$

$$\prod \lambda_f^{-1} \lambda_c^{-1} (t_c/R_c)^{-2/3} (k_1 k_2)^{-2/3} \leq 1 \quad (\text{FW}) \quad (12b)$$

$$\prod 2\lambda_c^{-1} (t_c/R_c)^{-1} (1 - \cos \theta_c) (\tau_{\max}/E)^{-1} \leq 1 \quad (\text{CF}) \quad (12c)$$

$$\prod \lambda_c^{-1} (t_c/R_c)^{-3} k_3 \leq 1 \quad (\text{CB}) \quad (12d)$$

where  $k_1 = \left( \frac{3}{2(1 + \nu_c^*)(3 - \nu_c^*)} \right)$ , and  $k_2 = \left( \frac{\theta_c}{2(1 - \cos \theta_c) \sin \theta_c} \right)$  and  $k_3 = (6/f_1 \pi^2)(1 - \cos \theta_c) \theta_c^2 (1 - \nu^2)$ .

Any failure constraint is active when its value is equal to 1. Note, intracellular buckling mode will be discussed later.

##### 4.1. Solution methodology

The optimum weight is obtained at the confluence of any three failure mechanisms. Therefore, four such combinations are possible: (1) FF–CF–CB, (2) FW–CF–CB, (3) FF–FW–CF, and (4) FF–FW–CB. A generic approach to this problem is to express any three geometric parameters in terms of the fourth one, say  $\lambda_c$ , using the three active constraints. Then the weight  $w$  given by Eq. (11) becomes a function of  $\lambda_c$  only and the optimum  $\lambda_c$  is given by  $dw/d\lambda_c = 0$ . The solution is admissible, if the remaining constraint is satisfied; otherwise the solution is inadmissible. The minimum weight derived from these four combinations is the optimum. In the present example, analytical expressions become quite complicated and implicit in nature because of the presence of  $\theta_c$ . Therefore,  $\theta_c$  is considered as a fixed parameter and its sensitivity on optimal weight has been studied later. As a result, the four-variable optimisation problem is reduced to a three-variable optimisation problem. However, a complete numerical route may be used for calculating the optimum values of  $\theta_c$  and other parameters that lead to the optimum weight.

Three-parameter optimisation is not very straightforward as the scaling of the variables  $\lambda_f$  and  $\lambda_c$  are the same in (12a) and (12b). Furthermore,  $\lambda_c$  has the same scaling in (12c) and (12d). Therefore, for combinations (1) and (2),  $t_c/R_c$  values are calculated equating

constraints (12c) and (12d). On the other hand, for combinations of (3) and (4),  $t_c/R_c$  values are calculated using respective constraints (12c) and (12d). Based on the three-parameter optimisation, closed form expressions of the geometric parameters are developed that would lead to the minimum panel weight for various combinations of constraints, shown in Table 1. For any prescribed loading, the optimum weight value can be calculated using Eq. (11), with the values of geometrical parameters evaluated using the expressions given in Table 1. However, instead of only calculating the optimum values, values of the geometric parameters and panel weight are calculated for a wide range of  $\lambda_c$  values because it gives better insight of the failure behaviour.

#### 5. Results and discussion

The optimisation has been performed in the *MATLAB* [27] environment for the sandwich panels with faces and hollow core made of 3-ply veneer. Each ply thickness is 0.6 mm, with a total thickness  $\sim 1.8$  mm. Experimental results show that for comparable densities, the specific shear strength of the hollow core 11.8 kN·m/kg is a lot better than that of the commercial PP honeycombs 5.45 kN·m/kg, but less than Nomex about 26 kN·m/kg. The cell wall material (veneer) properties are:  $E = 4.78$  GPa,  $\sigma_f = 59.87$  MPa,  $\tau_{\max} = 29.45$  MPa,  $\nu = 0.3$  and  $\rho = 520$  kg/m<sup>3</sup>. The value of core Poisson's ratio  $\nu_c^*$  is taken as 0.3. The value of  $\theta_c$  is 46°, which is the value of  $\theta_c$  for the manufactured core profile.  $t_c/R_c$  ratio for the core can vary widely from 0.005 to 0.25. As a result, the value of  $f_1$  in (4) varies between approximately 4.28 and 1.5 [24]. For a conservative design, the lower bound value of 1.5 is considered here. For this geometry, each cell wall was modelled as three layers using SHELL181 element. Finite element analysis using ANSYS shows that the shear stress variation between the layers is less than 5%. This justifies our assumption that the shear stress can be considered as uniform across the cell wall. As an example, optimisation results corresponding to load index  $V^2/EM = 1 \times 10^{-4}$  is presented first to explain the generic features of the plot.

Fig. 3a is a plot for the weight index  $w$  for various values of  $\lambda_c$  for the four combinations of active constraints. Fig. 3b zooms on Fig. 3a to show the nature of the curves in detail. The bottom-most dotted line in Fig. 3a representing combination, FW–CF–CB, is always an *inadmissible solution*, and hence omitted in Fig. 3b. The plot shows that for FF–CF–CB and FF–FW–CB combinations, the required weight reduces with an increase in core depth, until it reaches the lowest (optimum) value and then increases gradually. On the other hand, the weight indicated by FF–FW–CF combination progressively reduces and does not indicate any optimum. These three curves converge at point P and then diverge again. However, until point P, FF–FW–CF combination produces an admissible solution, whereas FF–FW–CB produces an inadmissible solution. This reverses after point P when FF–FW–CB turns out to be an admissible combination and FF–FW–CF becomes an inadmissible combination. On the contrary, FF–CF–CB combination always produces an admissible solution. Though the weight values as predicted by the two admissible combinations are close until point P, FF–FW–CF predicts higher values relative to the FF–CF–CB combination. After point P, FF–FW–CB predicts lower weight than FF–CF–CB and reaches a minimum value (point R in the figure) and gradually increases again. Similar trend is observed for FF–CF–CB combination as it also reaches a minimum (point Q) and then increases again. Because FF–FW–CF does not lead to any optimum weight, expressions of the geometric parameters shown in Table 1 would lead to the weight at point P, the lowest weight possible by this combination. The weight corresponding to R is the *global minimum* panel weight for load index  $1 \times 10^{-4}$ . For the current set of parameters, the weight and the associated geometric parameters

**Table 1**  
Closed form expressions for the optimum geometric parameters that produce the minimum panel weight for various combinations of constraints.

Combination No.	$t_c/R_c$	$\lambda_c$	$\lambda_f$
1	$\theta_c/\pi\sqrt{2(1-\nu_c^2)(\tau_{max}/E)}$	$\sqrt{2}\prod[(t_c/R_c)^{-1/2}k_2^{-1/2}(\tau_{max}/E)^{-1/2}]$	$\prod\lambda_c^{-1}(\tau_{max}/E)^{-1}$
2	$\theta_c/\pi\sqrt{2(1-\nu_c^2)(\tau_{max}/E)}$	$\sqrt{2}\prod[(t_c/R_c)^{-5/6}k_1^{-1/6}k_2^{-2/3}]$	$\prod\lambda_c^{-1}(t_c/R_c)^{-2/3}(k_1k_2)^{-1/3}$
3	$\theta_c/\pi\sqrt{2(1-\nu_c^2)(\tau_{max}/E)}$	$2\prod[(t_c/R_c)^{-1}(1-\cos\theta_c)(\tau_{max}/E)^{-1}]$	$\prod\lambda_c^{-1}(\tau_{max}/E)^{-1}$
4	$(\prod\lambda_c^{-1}k_3)^{1/3}$	$(3\prod^{2/3}k_2^{-1}k_3^{-1/3}(\tau_{max}/E)^{-1})^{3/5}$	$\prod\lambda_c^{-1}(\tau_{max}/E)^{-1}$

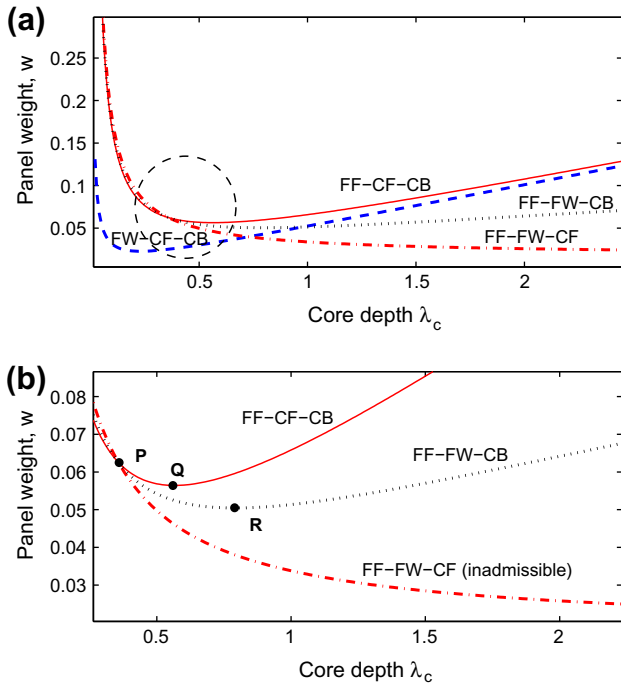


**Fig. 3.** (a) The panel weight values are plotted as a function of core depth  $\lambda_c$  for load index  $V^2/EM = 1 \times 10^{-4}$ , and parameter  $\theta_c = 46^\circ$ . Weight trajectories as calculated by four combinations of failure constraints are shown. (b) The circled portion in (a) is zoomed in to show the optimum (minimum) weight values at points Q and R, predicted by combinations FF-CF-CB and FF-FW-CB, respectively. Three curves converge at P and then diverge again.

corresponding to points P, Q and R are shown in Table 2. Full four-parameter optimisation calculations were also performed using MATLAB optimisation toolbox and the results are presented in Table 2 for comparison. The table shows that the global minimum weight as calculated by MATLAB is only 6% lower than that predicted by simplified three-parameter optimisation (point R). Furthermore, for FF-CF-CB and FF-FW-CF combinations, the weight values predicted by MATLAB calculations are lower than the respective optimised (three-parameter) values.

Calculations show that before point P, FF-FW-CF and FF-FW-CB produce admissible and inadmissible solutions, respectively. To explore this in detail, core  $t_c/R_c$  values are plotted as a function

of core depth  $\lambda_c$ , for load index  $1 \times 10^{-4}$ , in Fig. 4. For FF-FW-CF, core  $t_c/R_c$  values are calculated using constraint (Eq. (12c)) equated to 1, and the resultant curve (solid line) is the shear fracture (CF) curve. On the other hand,  $t_c/R_c$  values determined using Eq. (12d) as an active constraint are represented by the shear buckling (CB) curve, the dotted line. Fig. 4 shows that for lower core depth, the core failure is governed by shear fracture rather than by shear buckling. However, this reverses beyond the intersection point and shear buckling becomes the governing failure mode. As a result, CF and hence, FF-FW-CF combination produces admissible solution before the intersection point, provided face fracture and wrinkling criteria (12a) and (12b) are met. In contrast, CB and therefore, FF-FW-CB becomes an inadmissible combination even if face fracture and wrinkling criteria are satisfied. Beyond the intersection point, cell wall buckling becomes the governing failure mode and hence, FF-FW-CB only provides the admissible solution. Therefore, the intersection point represents the  $t_c/R_c$  value associated to P in Fig. 3b. This value can be calculated using  $t_c/R_c = \theta_c/\pi\sqrt{2(1-\nu_c^2)(\tau_{max}/E)}$  as 0.027. This expression is obtained by equating (12c) and (12d) and eliminating  $\lambda_c$ , and is shown in Table 1. For these two combinations, substituting FF constraint (12a) in FW (12b) leads to  $t_c/R_c = 0.002$ . In Fig. 4, the horizontal line represents  $t_c/R_c = 0.002$ . Both the face wrinkling and fracture can be prevented for any loading if  $t_c/R_c = 0.002$ . For  $t_c/R_c \neq 0.002$ , either FF or FW would govern the failure. As FF and FW expressions have the same scaling ( $-1$ ) for  $\lambda_c$  and  $\lambda_f$ , for  $t_c/R_c < 0.002$ , the face thickness  $\lambda_f$  is to be evaluated according to FW (12b) as FW is the governing failure mode. On the other hand, for  $t_c/R_c > 0.002$ , face fracture would be critical and therefore, face thickness is to be designed using FF (12a). For most practical cases,  $t_c/R_c$  value is expected to be greater than 0.002. Therefore, in Table 1, the expressions of face thickness calculations are shown based on FF criterion, rather than FW.

The solutions obtained using combinations (1) and (2), FF-CF-CB and FW-CF-CB, indicate a balanced core design, as the core fails simultaneously by cell wall fracture and buckling. The corresponding value of  $t_c/R_c$  as calculated using the earlier expression  $t_c/R_c = \theta_c/\pi\sqrt{2(1-\nu_c^2)(\tau_{max}/E)}$  is 0.027. The expression shows that the value of  $t_c/R_c$  is constant for a prescribed set of material properties and  $\theta_c$ , and is independent of loading and other geometric parameters. For this  $t_c/R_c$  value, the admissible solution is obtained only for combination FF-CF-CB, and not for FW-CF-CB. This is due to the fact that for  $t_c/R_c > 0.002$ , face thickness  $\lambda_f$  calculated on the basis of face wrinkling cannot prevent face fracture

**Table 2**  
The minimum weight values and the associated geometric parameters as predicted by various combinations of active constraints using (i) three-parameter optimisation (closed form) and (ii) full four-parameter optimisation using MATLAB. (M) denotes the MATLAB values. The load index,  $V^2/EM = 1 \times 10^{-4}$ .

Point No.	Combinations	Minimum panel weight, $w$	Core depth, $\lambda_c$	Core, $t_c/R_c$	Face thickness, $\lambda_f$	$\theta_c$ ( $^\circ$ )
P	FF-FW-CF	0.063	0.360	0.027	0.022	46
P	FF-FW-CF (M)	0.051	0.565	0.0485	0.014	82
Q	FF-CF-CB	0.056	0.560	0.027	0.014	46
Q	FF-CF-CB (M)	0.051	0.565	0.0485	0.014	82
R	FF-FW-CB	0.051 (global minimum)	0.790	0.021	0.010	46
R	FF-FW-CB (M)	0.048 (global minimum)	0.830	0.033	0.001	67

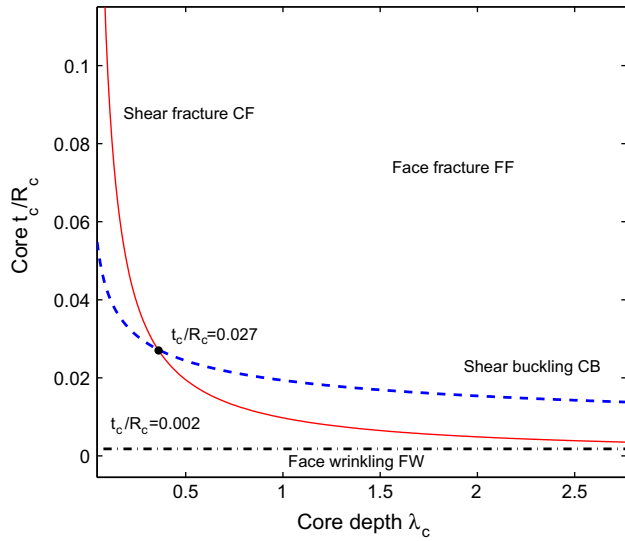


Fig. 4. Plot of core  $t_c/R_c$  values as a function of core depth  $\lambda_c$ . The load index is  $1 \times 10^{-4}$ , and parameter  $\theta_c = 46^\circ$ . The core fails simultaneously by cell wall fracture and buckling for  $t_c/R_c$  ratio of 0.027.

and hence, FW–CF–CB is not a viable solution for  $t_c/R_c = 0.027$ . Because of the same scaling ( $-1$ ) for  $\lambda_c$  and  $\lambda_f$  in FF, higher value of face thickness is required for lower core depth and that increases the weight, even though the  $t_c/R_c$  component remains the same.

Four failure criteria that have been used so far are the most significant ones. However, intracellular buckling mode has also been investigated. For  $t_c/R_c > 0.002$ , face thickness is governed by FF criterion. Therefore, face fracture and intracellular buckling are considered here as the dominant failure modes. However, for  $t_c/R_c < 0.002$ , face wrinkling and intracellular buckling need to be considered. Assuming that face fracture and intracellular buckling occur simultaneously, Eq. (10) can be reduced to the following form (using (6)),

$$\left(\frac{\lambda_{Rc}}{\lambda_f}\right)^2 = \frac{1}{8} (\sigma_f/E)^{-1} (1 - \nu^2)^{-1} (1 - \cos \theta_c)^{-2} \quad (13)$$

Note that Eq. (13) is independent of loading and core depth. To ensure that this failure would not occur before face fracture, the preceding relationship would pose a limit on the cell size  $\lambda_{Rc}$  for a given face thickness  $\lambda_f$  or vice versa. For the current set of material and geometric parameters, Eq. (13) can be reduced to  $\lambda_{Rc} = 10.85\lambda_f$ , which is the upper bound of the allowable cell sizes associated to a particular face thickness. The cell size governed by the radius of curvature  $R_c$ , is limited by the manufacturing constraint. Therefore,  $R_c$  could be the limiting factor, and would, in turn, dictate the face thickness. For the reported sample,  $\lambda_{Rc} = 0.27$ ; considering this as the upper bound,  $\lambda_f$  must be  $\geq 24.9 \times 10^{-3}$ . For  $\lambda_f < 24.9 \times 10^{-3}$ , face will buckle before fracture, and hence, intracellular buckling would be critical. Since, the lower bound of face thickness is very low, for most practical cases intracellular buckling is not critical, unless the cell is too large, or the face thickness is too low.

In the case of core-face delamination, the compressive face buckling load will depend on various factors including core stiffness, face thickness, debonding length and bond quality [28]. Our analysis assumes that there is no delamination between the face and skin (including the multi-layer face sheet delamination) and attempts to optimise the panel geometry. For the experimental part also (not reported here), sufficiently strong glue and improved application methods are being used to avoid delamination. Therefore, the design will be conservative considering the other four failure criteria.

However, it is to be noted that the load carrying capacity of the panel will be adversely affected in the case of delamination.

The minimum panel weight is predicted for a wide range of loading and is plotted in Fig. 5. The solid and the dashed line above it, are the trajectories of points Q and R (refer to Fig. 3b), representing the lowest weight as predicted by FF–CF–CB and FF–FW–CB combinations, respectively. It can be seen from Fig. 3 that for any load, FF–FW–CF combination does not indicate any optimum, but predicts lowest admissible weight at P. Therefore, the trajectory of P is also shown, the topmost line in the figure. For lower loads, R trajectory (FF–FW–CB) determines the global minimum. For any load, the Q values are now higher yet close to the respective R values. However, with further increase in loading beyond point S, Q trajectory (FF–CF–CB) represents the optimum weight and R trajectory becomes inadmissible solution. This happens because at higher loads, P lies on the right of R and FF–FW–CB is an admissible combination only before P. The three trajectories converge together at point S. Thus at S, the panel can fail simultaneously by all the failure modes. The associated transition load index and weight values are  $5.46 \times 10^{-4}$  and 0.14, respectively. The corresponding geometric parameters are:  $\lambda_c = 1.985$ ,  $\lambda_f = 0.022$ ,  $t_c/R_c = 0.027$ . Note that P trajectory always predicts relatively higher weight than Q and R, except at point S.

Fig. 6 represents the optimal values of the geometric parameters of the panel: core depth,  $t_c/R_c$  for the core and face thickness for a wide range of loading. The first and third plot shows that the core depth along with the face thickness increases with the load, because of their inverse scaling ( $-1$ ). For both of them, the slope of the curve changes at load index of  $5.46 \times 10^{-4}$  as the combination of active constraints changes from FF–FW–CB to FF–CF–CB. This is the same load index beyond which the minimum weight is governed by FF–CF–CB, instead of FF–FW–CB before the loading (as shown in Fig. 5). For loadings lower than  $5.46 \times 10^{-4}$ ,  $t_c/R_c$  values are lower than 0.027. However, beyond this loading, FF–CF–CB dictates the optimum solution and therefore,  $t_c/R_c$  value remains constant at 0.027 as shown in the second plot.

### 5.1. Sensitivity of half angle $\theta_c$

The values of  $\theta_c$  were varied for  $30^\circ$ ,  $60^\circ$  and  $90^\circ$ , and the corresponding minimum weight values were calculated for a wide range of loading.  $\theta_c = 90^\circ$  is a special case of the geometry made of half circles with  $R = h_c/2$ . Fig. 7 shows a plot of minimum weight vs. load index with  $\theta_c$  as a parameter. The general trend of all curves remains same as was observed for  $\theta_c = 46^\circ$  in Fig. 5. Beyond a certain loading, the slope of each curve changes when the governing combination of the active constraints changes from FF–FW–CB to

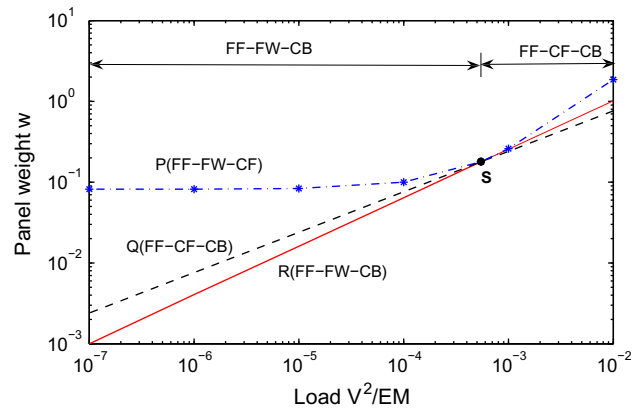


Fig. 5. Design map showing minimum weight of the panel for a wide range of loading for various combinations of failure constraints. Three curves converge together at  $V^2/EM = 5.46 \times 10^{-4}$ . The corresponding panel weight  $w = 0.14$ .

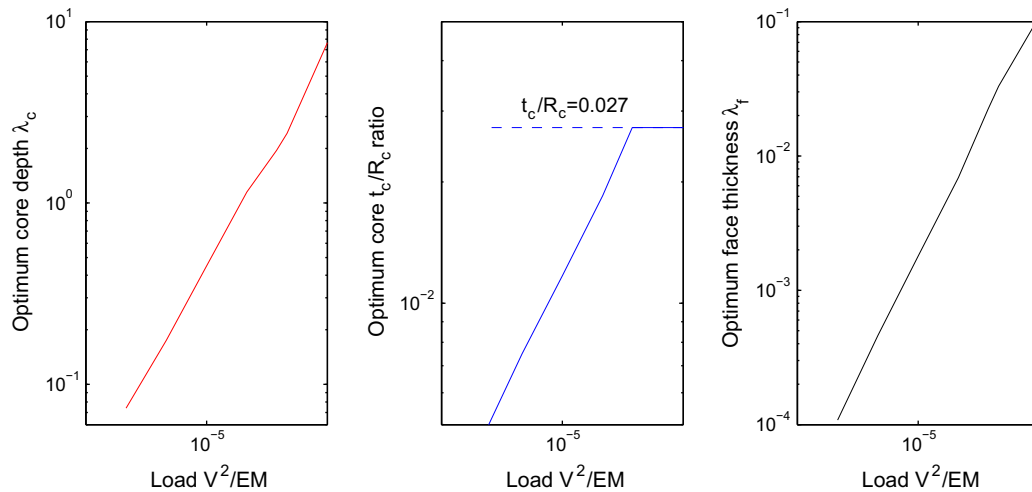


Fig. 6. Design map indicating the optimum values of the geometric parameters: core depth  $\lambda_c$ ,  $t_c/R_c$  of the core and face thickness  $\lambda_f$  for a wide range of loading.

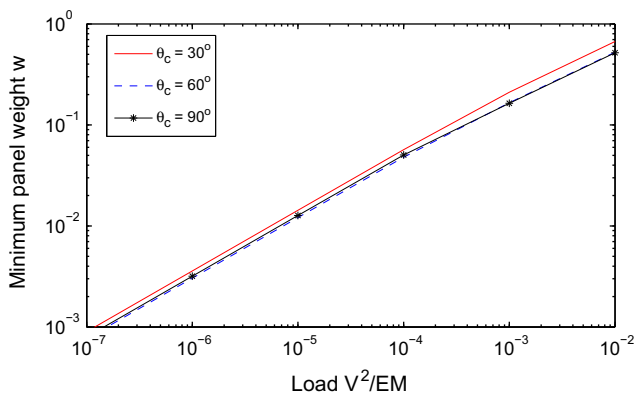


Fig. 7. Plot of minimum weight vs. loading with  $\theta_c$  as a parameter. The variations in panel weight for different values of  $\theta_c$  are not very significant.

FF–CF–CB. The plot shows that for any loading, the difference in weight for various values of  $\theta_c$  is not that significant. For instance, corresponding to load index  $1 \times 10^{-4}$ , the minimum weight for  $\theta_c = 46^\circ$ ,  $60^\circ$  and  $90^\circ$ , are 0.051, 0.048, 0.050, respectively. *MATLAB* calculations were performed for two loading cases:  $1 \times 10^{-4}$  and  $1 \times 10^{-3}$ , above and below the transition loading, respectively. The results show that for  $1 \times 10^{-4}$ ,  $\theta_c = 67^\circ$  gives the minimum weight for FF–FW–CB; whereas for  $1 \times 10^{-3}$ ,  $\theta_c = 46^\circ$  predicts the minimum weight for FF–CF–CB. Interestingly,  $\theta_c = 46^\circ$  was used for the optimisation calculation. Lower sensitivity of  $\theta_c$  on minimum weight calculation justifies three-parameter optimisation approaches with a judicious choice of  $\theta_c$  value.

There may be practical limitations of manufacturing a fully optimised panel. For example, it is easier to control core depth and face thickness to some extent, but it is quite difficult to achieve the targeted  $t_c/R_c$  ratio as reducing the cell wall thickness  $t_c$  may not always be possible. The allowable value of  $R_c$  is guided by the manufacturing constraints and is also dependent on  $t_c$ . However, increasing  $R_c$  would reduce the  $t_c/R_c$  ratio (for same  $t_c$ ), and produce larger cells, thus making the panel more prone to intracellular buckling type failure.

## 6. Conclusions

To meet the growing demand of replenishable, lightweight and strong materials, novel hollow core sandwich panels have been manufactured using 3-ply veneer. The mechanics of a representa-

tive unit cell when subjected to out-of-plane shear forces was analysed and the expressions for the failure loads have been developed. Based on the failure criteria of a sandwich panel, an optimisation formulation has been achieved for predicting the minimum weight of the wood veneer sandwich panel for a prescribed bending load. The four-parameter optimisation problem was reduced to a three-parameter problem by choosing  $\theta_c$  as a fixed parameter. A sensitivity study has been performed to show that the value of  $\theta_c$  does not influence the panel weight significantly. Furthermore, it has been observed that the optimum weight calculated by the full four-parameter optimisation is slightly lower than that predicted by the simplified three-parameter optimisation. Hence, the closed form expressions of the geometric parameters developed in this work can be used to predict their optimum values to achieve the minimum panel weight. Design maps are shown to indicate the minimum panel weight and the corresponding geometric parameters for a wide range of loading. Relationships between the various active failure modes have been explored. Note, the developed analysis is general enough to be applicable for sandwich panels with similar hollow cores made of other materials.

## Acknowledgement

The authors wish to thank Foundation for Research Science and Technology New Zealand for providing financial support for this research.

## References

- [1] Kelsey S, Gellatly RA, Clark BW. The shear modulus of foil honeycomb core. *Aircraft Eng* 1958;30:294–302.
- [2] Gibson LJ, Ashby MF. *Cellular solids: structure and properties*. 2nd ed. Cambridge: Cambridge Univ. Press; 1997.
- [3] Penzien J, Didriksson T. Effective shear modulus of honeycomb cellular structures. *AIAA J* 1964;2(3):531–5.
- [4] Shi G, Tong P. Equivalent transverse stiffness of honeycomb cores. *Int J Solids Struct* 1995;32(10):1383–93.
- [5] Xu XF, Qiao P, Davalos JF. Transverse shear stiffness of composite honeycomb core with general configuration. *J Eng Mech* 2001;127(11):1144–51.
- [6] Hohe J, Becker W. A mechanical model for two dimensional cellular sandwich cores with general geometry. *Comput Mater Sci* 2000;19:108–15.
- [7] Hohe J, Becker W. An energetic homogenisation procedure for the elastic properties of general sandwich cores. *Composites Part B* 2001;32:185–97.
- [8] Chen A, Davalos JF. A solution including skin effect for stiffness and stress field sandwich honeycomb core. *Int J Solids Struct* 2005;42(9–10):2711–39.
- [9] Grediac M. A finite element study of the transverse shear in honeycomb cores. *Int J Solids Struct* 1993;30(13):1777–88.

- [10] Zhang J, Ashby MF. The out-of-plane properties of honeycombs. *Int J Mech Sci* 1992;34(6):475–89.
- [11] Wicks N, Hutchinson JW. Optimal truss plates. *Int J Solids Struct* 2001;38(30–31):5165–83.
- [12] Wicks N, Hutchinson JW. Performance of sandwich plates with truss cores. *Mech Mater* 2004;36(8):739–51.
- [13] Zok FW, Rathbun HJ, Wei Z, Evans AG. Design of metallic textile core sandwich panels. *Int J Solids Struct* 2003;40(21):5707–22.
- [14] Zok FW, Waltner SA, Wei Z, Rathbun HJ, McMeeking RM, Evans AG. A protocol for characterizing the structural performance of metallic sandwich panels: application to pyramidal truss cores. *Int J Solids Struct* 2004;41(22–23):6249–71.
- [15] Valdevit L, Wei Z, Mercer C, Zok FW, Evans AG. Structural performance of near-optimal sandwich panels with corrugated cores. *Int J Solids Struct* 2006;43(16):4888–905.
- [16] Rathbun HJ, Zok FW, Evans AG. Strength optimisation of metallic sandwich panels subject to bending. *Int J Solids Struct* 2005;42(26):6643–61.
- [17] Wei Z, Zok FW, Evans AG. Design of sandwich panels with prismatic cores. *J Eng Mater Technol ASME* 2006;128:186–92.
- [18] Cote F, Deshpande VS, Fleck NA, Evans AG. The compressive and shear responses of corrugated and diamond lattice materials. *Int J Solids Struct* 2006;43(20):6220–42.
- [19] Allen HG. Analysis and design of structural sandwich panels. Oxford: Pergamon Press; 1969.
- [20] Zenkert D. An introduction to sandwich construction. London: EMAS; 1995.
- [21] Vinson JR. The behaviour of sandwich structures of isotropic and composite materials. Pennsylvania: Technomic Publishing Company Inc.; 1999.
- [22] Noor AK, Burton WS, Bert C. Computational models for sandwich panels and shells. *Appl Mech Rev ASME* 1996;49(3):155–99.
- [23] Srinivasan N, Bhattacharyya D, Jayaraman K. Profile production in multi-veneer sheets by continuous roll forming. *Holzforschung* 2007;62:453–60.
- [24] Timoshenko SP, Gere JM. Theory of elastic stability. 2nd ed. New York: McGraw-Hill; 1961.
- [25] Niu K, Talreja R. Modelling of wrinkling in sandwich panels under compression. *J Eng Mech ASCE* 1999;125(8):875–83.
- [26] Ashby MF, Evans AG, Fleck NA, Hutchinson JW, Wadley HNG. Metal foams: a design guide. Boston: Butterworth Heinemann; 2000.
- [27] MATLAB 6.7, User's guide, The Mathworks, Inc., Natick, MA; 2008.
- [28] Niu K, Talreja R. Buckling of a thin face layer on Winkler Foundation with debonds. *J Sandwich Struct Mater* 1999;1:259–78.